Journal of Hazardous Materials 170 (2009) 184–190

Contents lists available at ScienceDirect

Journal of Hazardous Materials

journal homepage: www.elsevier.com/locate/jhazmat

Photocatalytic degradation of basic blue 9 by CoS nanoparticles supported on AlMCM-41 material as a catalyst

Sh. Sohrabnezhad[a,*], A. Pourahmad[b], E. Radaee[a]

[a] Department of Chemistry, Faculty of Science, University of Mohaghegh Ardabili, Ardabil, Iran
[b] Department of Chemistry, Faculty of Science, Islamic Azad University, Rasht Branch, Rasht, Iran

ARTICLE INFO

Article history:
Received 3 January 2009
Received in revised form 26 April 2009
Accepted 28 April 2009
Available online 3 May 2009

Keywords:
Photocatalyst
Methylene blue
MCM-41
X-ray diffraction
Diffuse reflectance spectroscopy

ABSTRACT

In this investigation photocatalytic degradation of basic blue 9 or methylene blue (MB) as color pollutants was studied. Cobalt sulfide was supported on AlMCM-41 material using ion-exchange method. The results show that CoS/AlMCM-41 is an active photocatalyst. The catalyst is characterized by X-ray diffraction (XRD) UV–vis diffused reflectance spectra (UV–vis DRS) and scanning electron microscopy (SEM) techniques. The maximum effect of photodegradation was observed at 7 wt% CoS/AlMCM-41. Pseudo-first order reaction with $k = 0.032$ was observed for the photocatalytic degradation reaction. The effect of some parameters such as pH, amount of photocatalyst and initial concentration of dye were also examined. The effect of dosage of photocatalyst was studied in the range 0.04–1.2 g/L. It was seen that 0.8 g/L of photocatalyst is an optimum value for the dosage of photocatalyst. In the best conditions, the degradation efficiency was obtained 0.32 ppm for MB dye.

1. Introduction

Environmental problems associated with hazardous wastes and toxic water pollutants have attracted much attention. Among them, organic dyes are one of the major groups of pollutants in wastewaters produced from textile and other industrial processes [1–4]. Among various physical, chemical and biological techniques for treatment of wastewaters, heterogeneous photocatalysis has been considered as a cost-effective alternative for water remediation [5]. The superiority of photocatalytic technique in wastewater treatment is due to its advantages over the traditional techniques, such as quick oxidation, no formation of polycyclic products, oxidation of pollutants in the ppb range. Photocatalysis is a process by which a semiconductor material absorbs light of energy more than or equal to its band-gap, thereby generating electrons and holes which can further generate free radicals in the system to oxidize the substrate. The resulting free radicals are very efficient oxidizers of organic matter [6,7].

The photocatalytic treatment of wastes containing dyes has also been widely reported in the literature. In most cases, TiO_2 was used as a famous photocatalyst, whereas, the other semiconductors such as metal sulfides were less used especially in the dimensions of nano-scale [8–12].

Nano-scale semiconductor particles possess higher surface area to volume ratio than their bulk counter parts, and thus allow for greater photon adsorption on the photocatalyst surface [5,12,13].

Moreover, recombination of the electron-hole pair within the semiconductor particle is drastically reduced as particle size decreases. With decreasing the particle size of semiconductor to nanometer size scale, the band-gap energy increased greatly, this in turn led to higher redox potentials in the system. Therefore, the nano-scale semiconductor is expected to have higher photocatalytic activity than its bulk.

One of the attractive research fields in recent years is synthesis of various sizes and shapes of semiconductor materials nanoparticles. The goal of these activities is improving the performance and utilization of nanoparticles in various applications from sensing devices to photonic materials in molecular electronics and to advanced oxidation techniques (AOTs). The size and shape dependent optical and electronic properties of these nanoparticles make an interesting case for exploiting them in light induced chemical reaction.

The main drawbacks are the need for complex filtration procedures and the high turbidity that decreases the radiation flux. Such problems have motivated the development of supported photocatalysts in which semiconductors are immobilized on different adsorbent materials. In this context, molecular sieves have attracted greater attention due to their adsorption capacity that helps in pooling the pollutants to the vicinity of the semiconductors surface and also leads to faster degradation [6,14,15]. Molecular sieves offer excellent control of size distribution and morphology through

* Corresponding author. Tel.: +98 451 5517137; fax: +98 451 5514701.
E-mail address: sohrabnezhad@uma.ac.ir (Sh. Sohrabnezhad).

0304-3894/$ – see front matter © 2009 Elsevier B.V. All rights reserved.
doi:10.1016/j.jhazmat.2009.04.108

the main pulsation of the wet chemical processing parameters. Microporous molecular sieves have been widely used for hosting nanoparticles, but they are limited to pore opening of less than 1 nm [16]. The recent discovery of mesoporous MCM-41 offers a possibility for synthesizing 3D heterostructures in a previously inaccessible size range, by inclusion chemistry [17]. MCM-41 is a porous amorphous silica material with a hexagonal honeycomb structure that can be synthesized with controllable pore diameter in the range 2–10 nm. Corma [18] has reported that calcined AlMCM-41, with aluminum incorporated into the framework of the MCM-41, exhibited an acidity of medium strength comparable to that of USY zeolite. AlMCM-41 material was used for ion-exchange reaction with cations.

This paper reports a simple route for the preparation of nanoparticles of cobalt sulfide into mesoporous AlMCM-41 material. The cobalt sulfide nanoparticles were synthesized by ion-exchange of the AlMCM-41 in aqueous suspension. The CoS/AlMCM-41 materials are used as photocatalyst in degradation of methylene blue as organic dyes are studied to achieve degradation efficiency of dye near 95%.

Methylene blue is a heterocyclic aromatic chemical compound with molecular formula $C_{16}H_{18}ClN_3S$. It has many uses in a range of different fields, such as biology or chemistry. It appears as a solid, odorless, dark green powder that yields a blue solution when dissolved in water at room temperature. This dye is stable, incompatible with bases, reducting agents and strong oxidizing agents. It is harmful if swallowed. It may be harmful if inhaled and if it comes in contact with skin as well as causes severe eye irritation and isinvestigated as a mutagen.

2. Experimental

2.1. Materials

The nitrate salts of cobalt ($Co(NO_3)_2$), from Merck, were used as source of metal ions and $Na_2S{\cdot}9H_2O$ (Merck) was used as source of sulfide ion. Hydrochloric acid and sodium hydroxide were applied for variation of PH of sample solutions. The dye of methylene blue (C.I. name: Basic Blue 9, $C_{16}H_{18}ClN_3S{:}3H_2O$) [Scheme 1] was purchased from Fluka company.

2.2. Preparation of AlMCM-41 material

The MCM-41 and AlMCM-41 materials were synthesized by a room temperature method with some modifications in the described procedure in literature [19]. We used tetraethylorthosilicate (TEOS: Merck, 800658) as a source of silicon and hexadecyltrimethylammonium bromide (HDTMABr; BOH, 103912) as a surfactant template for preparation of the mesoporous material. The molar composition of the reactant mixture is as follows:

$$SiO_2 : 1.6\,EA : 0.215\,HDTMA\,Br : 325\,H_2O$$

where EA stand for ethylamine. The MCM-41 prepared was calcined at 550 °C for 5 h to decompose the surfactant and obtain the white powder. This powder was used as the parent material to prepare AlMCM-41 free surfactant materials by ion-exchange method with 0.1 M of $Al_2(SO_4)_3{\cdot}18H_2O$ (Merck) solution. AlMCM-41 surfactant-free was used for loading the nanoparticles.

2.3. Preparation of CoS/AlMCM-41 catalysts

The solutions 0.05–0.25 M of $Co(NO_3)_2$ were prepared as precursors of the CoS semiconductor. For ion-exchange, 0.5 gr of AlMCM-41 powder was separately suspended in 25 ml solution of cobalt nitrate and stirred at room temperature for 5 h. After that, the sample was washed to remove unexchanged Co ions and then air-dried. Finally, sulfurizing of Co ions was carried out with 0.1 M Na_2S solution. To make the reaction with the S^{-2} ion, 0.5 gr of Co^{+2}-exchanged mesopore samples were added to 25 ml of 0.1 M Na_2S solution at a fixed temperature and magnetically stirred for 5 h. The samples were washed with deionized water and collected by filtration. The obtained samples were fine powders with grey color. The prepared samples are called CoS/AlMCM-41. The sample was stable at ambient condition. CoS of 2–20 wt% loading over AlMCM-41 support are prepared for their photocatalytic evolution.

2.4. Preparation of bulk CoS particles

For the sake of comparison, bulk CoS particles were prepared by a conventional precipitation method. In this method, an equimolar amount of Na_2S solution was added drop wise to a stirred solution of 0.1 M $Co(NO_3)_2$ resulting in the formation of bulk precipitates. The CoS precipitates were washed repeatedly with distilled water until free from S^{-2} ions, dried in an air-oven and then calcined at 500 °C for 4 h in air. The obtained sample was fine powder with dark color.

2.5. Characterization

Powder X-ray diffraction patterns of the samples were recorded using an X-ray diffractometer (Bruker D8 Advance) with Cu Kά radiation (λ=1.54 Å). The UV–vis diffused reflectance spectra (UV–vis DRS) obtained from UV–vis Scinco 4100 spectrometer with an integrating sphere reflectance accessory. $BaSO_4$ was used as reference material UV–vis absorption spectra were recorded using a shimadzu 1600 PC in the spectral range of 190–900 nm. Chemical analysis of the samples was done by energy dispersive X-ray analysis (EDX) joined a Philips XL30 scanning electron microscopy (SEM).

2.6. Procedures of photodegradation of methylene blue

Photodegrdation experiments were performed with a photocatalytic reactor system. This bench–scale system consisted of cylindrical Pyrex–glass cell with 1.0 L capacity, 10 cm inside diameter and 15 cm height. A 125 W mercury lamp (λ > 290 nm) was placed in a 5 cm diameter quartz tube with one end tightly sealed by a Teflon stopper. The lamp and the tube were then immersed in the photoreactor cell with a light path of 3.0 cm. The photoreactor was filled with 25 ml of 0.25–3.2 ppm of dye as pollutant and 0.04–2 g/L of CoS/AlMCM-41 as nanophotocatalyst. The whole reactor was cooled with a water-cooled jacket on its outside and the temperature was kept at 25 °C. All reactants in the reactions were

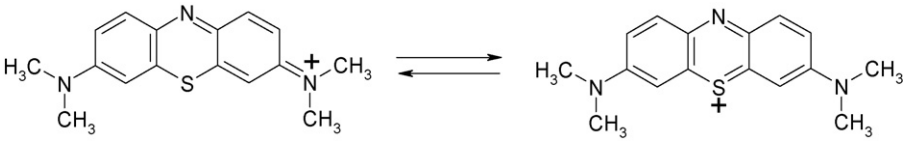

Scheme 1. Structure of methylene blue.

stirred using a magnetic stirrer to ensure that the suspension of the catalyst was uniform during the course of the reaction. To determine the percent of destruction of dyes, the samples were collected at regular intervals, and centrifuged to remove the nanocatalyst particles that exist as undissolved particles in the samples.

The wavelengths absorbance maximum (λ_{max}) of methylene blue is 664 nm. Therefore, photometric analysis of samples before and after irradiation can be used for measurement of the %*D* (degradation efficiency of dye). The absorption of solution and solid samples was measured by a UV–vis spectrophotometer shimadzu model 1600 PC and UV–vis diffused reflectance spectrometer UV–vis DRS Scinco model 4100, respectively. The decrease in absorbance value of samples at λ_{max} of dye after irradiation in a certain time interval will be shown as rate of decolorization and therefore, photodegradation efficiency of the dye as well as the activity of nanoparticles as photocatalyst. The decolorization and degradation efficiency have been calculated as:

$$\%D = 100 \times \frac{C_0 - C}{C_0}$$

where C_0 is the initial concentration of dye and C is the concentration of dye after irradiation in selected time interval.

In order to obtain maximum degradation efficiency, pH, concentration of dye and amount of photocatalyst were studied in amplitudes of 2–12, 0.25–3.2 ppm and 0.04–1.2 g/L, respectively. The experiments were carried out in the presence of CoS/AlMCM-41 mesoporous material for degradation of methylene blue dye.

3. Results and discussion

3.1. Characterization of CoS nanoparticles in AlMCM-41

The XRD pattern of AlMCM-41 support and CoS loading on the support are shown in Fig. 1. The AlMCM-41 support exhibited only a broad (1 0 0) peak at $2\theta = 2.2^\circ$, while other diffraction peaks corresponding to the (1 1 0) and (2 0 0) crystal plans were unresolved due to the large amount of aluminum incorporation [20]. In CoSAlMCM-41 sample the intensity of the (1 0 0) peak decreased. Decrease in the intensity should be attributed to the pore filling effects that can reduce the scattering contrast between the pores and the framework of AlMCM-41 sample.

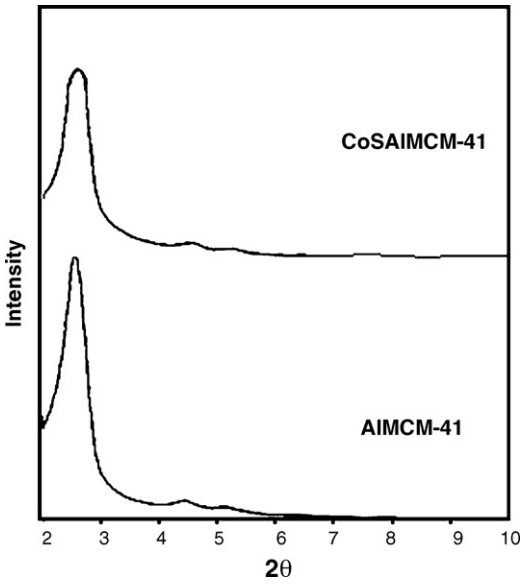

Fig. 1. X-ray diffraction patterns of the AlMCM-41 and 7 wt% CoS/AlMCM-41 catalyst.

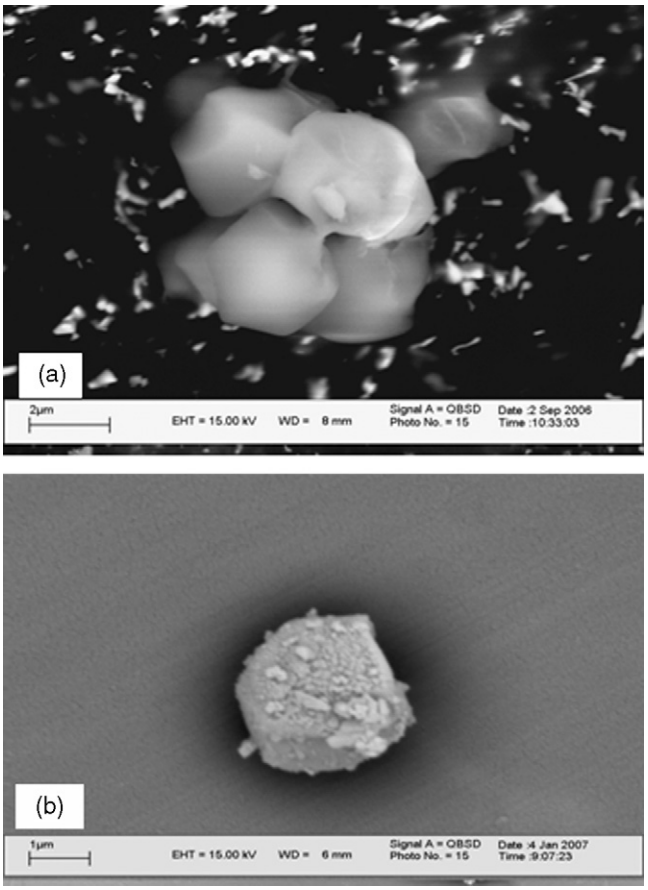

Fig. 2. Scanning electron micrograph of (a) AlMCM-41 and (b) 7 wt% CoS/AlMCM-41 catalyst.

The surface morphology of CoS nanoparticles has been studied by SEM. The SEM pictures of the CoS/AlMCM-41 sample and AlMCM-41 material are presented in Fig. 2. The SEM picture shows that lath shape of the AlMCM-41 molecular sieve is not affected by the CoS loading. The growth of fine particles of CoS in a regular pattern is observed on the surface of AlMCM-41 at CoS/AlMCM-41 sample.

The UV–vis diffuse reflectance spectra for CoS/AlMCM-41 (Fig. 3) show absorption edges of CoS at wavelengths of 320 and 350 nm. The CoSAlMCM-41 sample shows absorbance edges in the 290 and 360 nm. Absorption edges in 360 nm can explain the improved

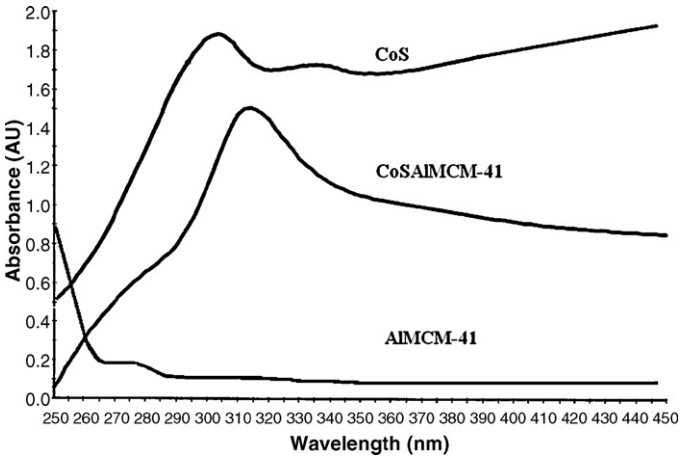

Fig. 3. Absorption spectra for the set of CoS samples.

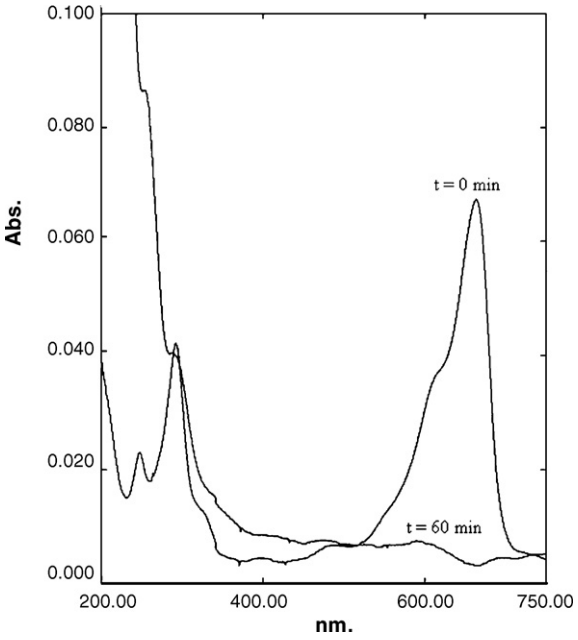

Fig. 4. Spectra change that occurs during the photocatalytic degradation of aqueous solution of methylene blue: pH 7, [7 wt% CoS/AlMCM-41] = 0.08 g/L, C_0 = 3.2 ppm.

photocatalytic activity of CoS/AlMCM-41 under UV region with respect to CoS (350 nm) sample. On the other hand, comparing the absorption edge of bulk CoS (320 nm) with that of CoS/AlMCM-41 (290 nm), it is seen that a blue shift is observed in CoS/AlMCM-41 sample. This phenomenon of blue shift of absorption edge is ascribed to a decrease in particle size of CoS. The estimated sizes of these CoS by using the Kayanuma model were 8 and 25 nm for CoS/AlMCM-41 and CoS bulk samples, respectively [21]. Meanwhile, diffuse reflectance spectrum for AlMCM-41 sample shows only absorption peaks at 270 nm (the same absorption edge 290 nm in CoS/AlMCM-41 sample) that related to extraframework aluminum in mesopore [22].

3.2. Photodegradation of dye using CoS/AlMCM-41 material

The time dependent electronic absorption spectrum of methylene blue dye during photo irradiation was presented in Fig. 4. After 60 min of irradiation under UV light in a CoS/AlMCM-41 suspension, 90% of dye was decomposed and decolorization of solution was observed. Besides, no new bands appear in the UV–vis region due to the reaction intermediates formed during the degradation process. The effects of UV irradiation, CoS and AlMCM-41 material on photodegradation of methylene blue are shown in Fig. 5. This figure indicates that in the presence of CoS (without AlMCM-41 and UV irradiation) 34% of dye degraded at the irradiation time of 70 min while it was 11.7% for AlMCM-41 and UV irradiation. These experiments demonstrated that both UV light and a photocatalyst, are needed for the effective degradation of methylene blue. It is well documented that the absorption of photons possessing energy equal to or higher than that of the semiconductor (3.58 eV for CoS in AlMCM-41) causes charge separation:

$$\mathrm{CoS} + h\nu \rightarrow \mathrm{CoS}(e^-) + \mathrm{CoS}(h^+)$$

The photogenerated holes may then react with adsorbed dye and oxidize the dye molecule by the formation of hydroxyl radicals. The photo-produced electrons in the conduction band react with the adsorbed oxygen to produced reactive radicals to yield the reactive oxygen species.

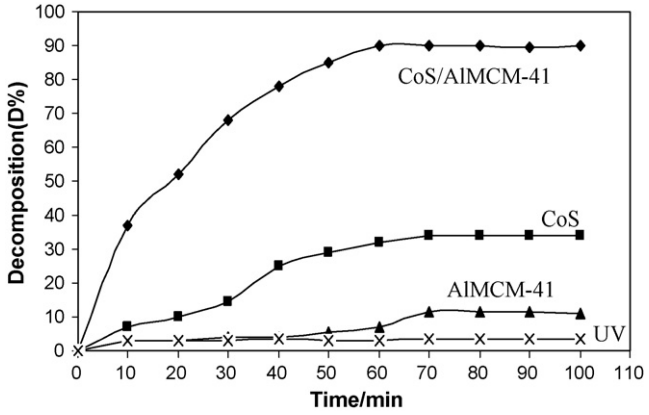

Fig. 5. Effect of UV light and different photocatalysts on photocatalytic degradation of methylene blue. C_0 = 3.2 ppm, [7 wt% CoS/AlMCM-41] = 0.08 g/L, pH 7.

To understand the role of support during the photocatalytic degradation of methylene blue, the amount of CoS available over 7 wt% CoS supported system is considered for the degradation activity and the studies are carried out using 0.8 g/L catalyst in 0.32 ppm methylene blue. From Figs. 4 and 5, it is observed that CoS supported system is showing higher rate of degradation than CoS or AlMCM-41 alone. This is due to the higher adsorption capacity and also OH radicals' availability. The 90% degradation of methylene blue on 7 wt% CoS/AlMCM-41 is observed within 60 min and it is 34% for CoS nanoparticles. The adsorption capacity of AlMCM-41 mesoporous enhances the chance of OH radicals attack on the adsorbed methylene blue molecules resulting faster degradation rates. Furthermore, CoS nanoparticles dispersion over AlMCM-41 mesoporous avoids particle–particle aggregation and light scattering by COS. Apart from all, the delocalizing capacity of AlMCM-41 mesoporous can effectively separate the electrons and holes produced during photo excitation of CoS, thus enhancing the photocatalytic efficiency [23].

3.3. Effect of variables' influence on degradation efficiency

3.3.1. Effect of catalyst concentration

In order to determine the optimal amount of photocatalyst, some experiments were performed at pH 7 by varying the amount of catalyst from 0.04 to 1.2 g/L. The effect of catalyst concentration on the rate of degradation is shown in Fig. 6. As seen, the optimum catalyst concentration for degradation of methylene blue dye is 0.8 g/L. It is observed that rate increases with increase in catalyst concentration from 0.04 to 0.8 g/L. This is probably due to increase in the number of CoS nanoparticles, that increases the number of photons absorbed and dye molecule absorbed. The increase in the

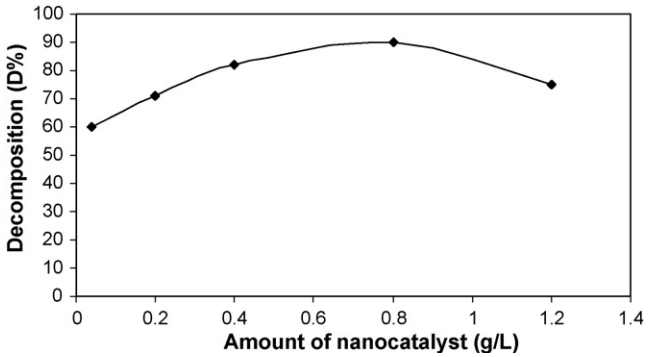

Fig. 6. Change in decomposition% of aqueous solution of methylene blue as a function of catalyst concentration: pH 7, C_0 = 3.2 ppm.

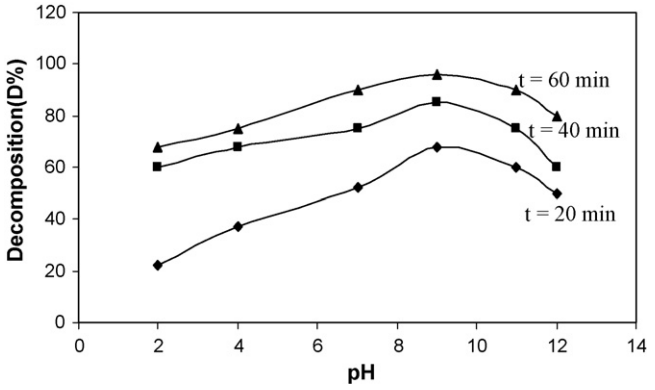

Fig. 7. Change in decomposition% aqueous solution of methylene blue as a function of pH: [7 wt% CoS/AlMCM-41] = 0.8 g/L, C_0 = 3.2 ppm.

catalyst concentration more than 0.8 g/L results in the decrease in degradation rate. This phenomenon may be explained by aggregation of CoS nanoparticles at high concentrations causing a decrease in the number of surface active sites and increase in opacity and light scattering of CoS nanoparticles at high concentration loading to decrease in the passage of irradiation through the sample.

3.3.2. Effect of PH

Photodegradation of dye (0.32 ppm) was studied in amplitude pH of 2.0–12 in the presence of CoS/AlMCM-41 catalyst (0.8 g/L). The results for irradiation time of 60 min are shown in Fig. 7. In all cases, the maximum degradation efficiency was obtained in alkaline pH 9 for methylene blue. In presence of CoS/AlMCM-41 and in pH 9, degradation efficiency 96% is obtained. Probably, the surface, of photocatalyst is positively charged in acidic solutions and negatively charged in alkaline solution. As a result, it is not surprise the increasing of the adsorption of dye molecules (with positive charge) on the surface of photocatalyst in alkaline solutions and thus the increasing of degradation efficiency of dye [24].

A low pH is associated with a positively charged surface which cannot provide hydroxyl group which is needed for hydroxyl radical formation. On the other hand, higher pH value can provide higher concentration of hydroxyl ions to react with the holes form hydroxyl radicals [25]. But, the degradation of dye is inhibited when the pH value is so high (pH > 9) because the hydroxyl ions compete with dye molecules in adsorption on the surface of photocatalyst [26].

In other words, at low pH, the adsorption of cationic dyes on the surface of photocatalysts decreased because the photocatalysts surface will be positively changed and repulsive forces are due to decreasing adsorption. Thus, the degradation efficiency will be decreased in acidic pH.

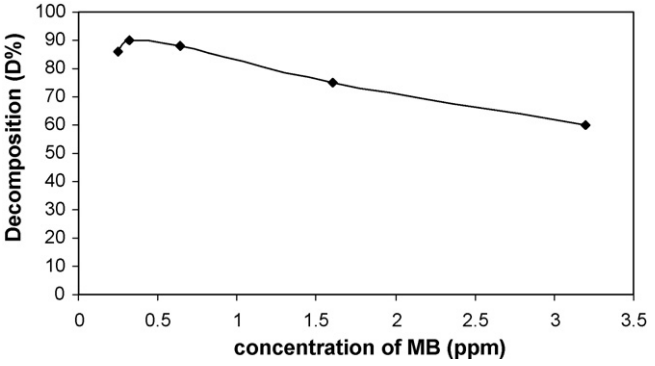

Fig. 8. Effect of concentration of dye on the photodegradation efficiency of methylene blue by 7 wt% CoSAlMCM-41 catalyst.

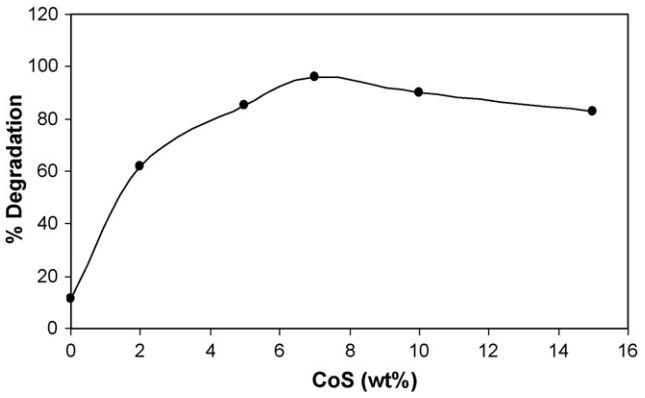

Fig. 9. Effect of composition of photocatalyst (wt% CoS) in mixture of CoS and AlMCM-41 on photocatalyst degradation of methylene blue after 60 min. C_0 = 0.32 ppm, [CoS/AlMCM-41] = 0.8 g/L, pH 7, T = 298 K.

3.3.3. Effect of concentration of dyes

The degradation efficiency of dye decreased with increasing the initial concentration of dye to more than 0.32 ppm. The results are shown in Fig. 8. The decrease in %*D* with increase in concentration of dye can be due to two reasons. With increasing the amounts of dye, the more of dye molecules will be adsorbed on the surface of the photocatalyst and the active sites of the catalysts will be reduced. Therefore, with increasing occupied space of catalyst surface, the generation of hydroxyl radicals will be decreased. Also, increasing concentration of dye can be lead to decreasing the number of photons that is arrived to the surface of catalysts. The more light isadsorbed by molecules of dye and the excition of photocatalyst particles by photons will be reduced. Thus, photodegradation efficiency diminished [27].

3.3.4. Effect of the composition of the supported photocatalyst

The effect of CoS loading on AlMCM-41 material is investigated with 2–20 wt% content and the results are depicted in Fig. 9. The effective decomposition of methylene blue after 60 min irradiation time was observed when the photocatalyst contained 7% CoS, prepared by using ion-exchange method. For comment of this result, we propose that the hydroxyl radical on the surface of nanoparticle CoS is easily transferred onto the surface of mesoporous material. This means that the organic pollutants, which have already been adsorbed on the mesoporous materials, have a chance to be degraded due to the appearance of hydroxyl radical, resulting in the enhancement of photodegradation performance of CoS/AlMCM-41. Experimental results show that about 7 wt% of CoS is the best condition to achieve the synergism between CoS and AlMCM-41. This synergetic effect may be due to the fact that the presence of AlMCM-41 is maintaining the molecules of dye near the photocatalyst as depicted in Fig. 10. The enhanced phtocatalytic activity over the composite CoS/AlMCM-41 is reflecting the beneficial adsorption properties of AlMCM-41. If decrease in the CoS in composition of photocatalyst is less than 7 wt% the rate of production reaction of the hydroxyl radical by CoS under UV irradiation is not enough to react with all the molecules of dye that are absorbed on the surface of AlMCM-41 and if there is increase in the CoS in the composition of photocatalyst, the adsorption ability of AlMCM-41 as compared with the rate of production reaction of hydroxyl radical with CoS under UV irradiation decrease.

3.4. Kinetics of photocatalytical degradation of methylene blue

Several experimental results indicated that the degradation rates of photocatalytic oxidation of various dyes over different catalysts fitted by first order kinetic model [28]. Fig. 11 shows the

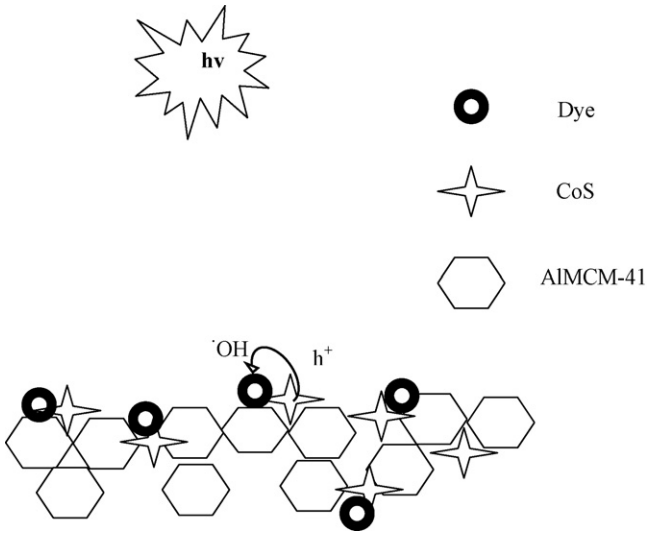

Fig. 10. Photocatalytic activity of CoS/AlMCM-41.

plot of $\ln([dye]_0/[dye])$ vs. irradiation time for methylene blue. The linearity of plot suggests that the photodegradation reaction approximately follows the pseudo-first order kinetics with $k = 0.0361$.

3.5. Recycling studies

Fig. 12 shows the reproducibility of CoSAlMCM-41 as nanoparticles for methylene blue photodegradation during a four-cycle experiment. Each experiment was carried out under identical concentration of 0.32 ppm of dye, 0.8 g/L of nanocatalyst, pH of 9, irradiation time of 60 min and at room temperature. After each degradation experiment, the concentration of dye was adjusted back to its initial value of 0.32 ppm. As seen from Fig. 12 a small and gradual decrease in the activity of nanocatalyst was observed at the first two cycles. The difference may be due to the accumulation of organic intermediate in the cavities and on surface of the mesoporous materials thus affecting the adsorption in turn reducing the activity. Nanocatalyst is calcined at 550°C for 2 h and reused; the rate of degradation is restored and is equivalent to fresh catalyst. Thus, the calcinations of the used catalyst are necessary in order to maintain the activity.

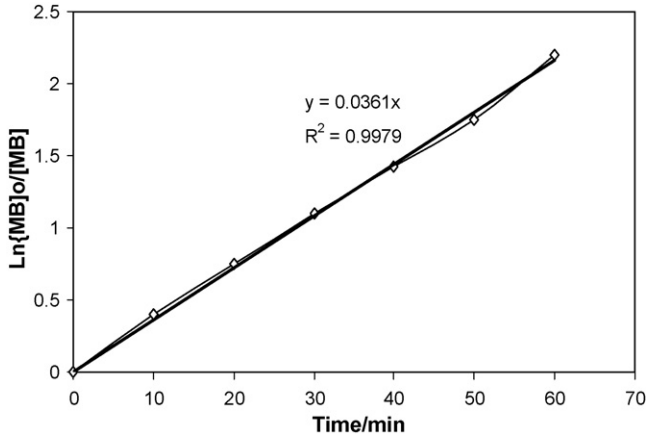

Fig. 11. Pseudo-first order linear transforms of disappearance of MB by photocatalyst under UV-irradiation, concentration of photocatalyst [7 wt% CoS/AlMCM-41] = 0.8 g/L, $T = 298$ K, pH 7.

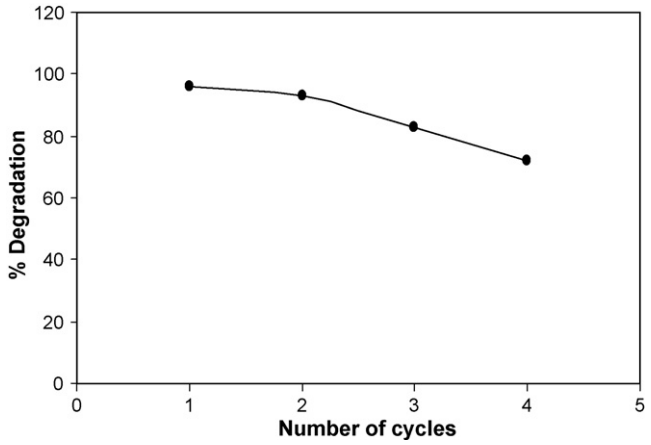

Fig. 12. Reproducibility of the 0.8 g/L it nanocatalysts for 0.32 ppm of methylene blue photodegradation in pH 9 and irradiation time of 60 min.

4. Conclusions

1. The ion-exchange method is an effective method for support of CoS on AlMCM-41.
2. A photocatalyst containing 7% CoS has the maximum efficiency on photodegradation of methylene blue.
3. The photodegradation conversion of methylene blue decreases with an increase in the initial concentration methylene blue.
4. pH is one of the main effecting factors and the optimum pH was obtained about 9.
5. The kinetics of photocatalytic degradation of methylene blue is of the pseudo-first order with $k = 0.0361$.

References

[1] Y. He, Synthesis of ZnO nano particles with narrow size distribution under pulsed microwave heating, Chin. Particuol. 2 (2004) 168–170.
[2] E. Hu, Y.Z. Wang, Decolorization and biodegradability of photocatatic treated azo dyes and wool textle wastwwater, Chemosphere 39 (1999) 2107–2115.
[3] J. Kiwi, C.M. Pulgarine, P.P. Gratzel, Beneficial effects of homogenous photofento pretreatment upon the biodegradation of anthraquionone sulfonate in waste water treatment, Appl. Catal. B: Environ. 3 (1993) 85–99.
[4] J. Li, Y. Xu, Y. Liu, D. Wu, Y. Sun, Synthesis of hydrophilic ZnS nanocrystal and their application in photocatalytic degradation of dye pollutants, Chin. Particul. 2 (2004) 266–269.
[5] M.R. Hoffman, S.T. Martin, W. Choi, D.W. Bahnemann, Environmental application of semiconductor photocatalysis, Chem. Rev. 95 (1995) 69–96.
[6] W. Panpa, P. Sujarid Worakan, S. Jinawath, Photocatalytic activity of TiO_2 ZSM-5 composites in the presence of SO_4^{-2} ion, Appl. Catal. B: Environ. 80 (2008) 271–276.
[7] Ch. Yogi, K. Kojima, N. Wable, H. Tokumoto, T. Takai, T. mizoguchi, H. Tamiaki, Photocatalytic degradation of methylene blue by TiO_2 film and Au particales TiO_2 composite film, Thin Solid Films 516 (2008) 5881–5884.
[8] S.K. Kansal, M. Singh, D. Sud, Studies on photodegradation of two commercial dyes in aqueous phase using different photocatalyst, J. Hazard. Mater. 141 (2007) 581–590.
[9] A. Orendorz, Ch. Ziegler, H. Gnaser, Photocatalytic decomposition of methylene blue and 4-chlorophenol on nanocrystalline TiO_2 films under UV illumination: A ToF-SIMS study, Appl. Surf 255 (2008) 1011–1014.
[10] S. Mozia, M. Toyoda, M. Inagoki, B. Tryba, A.W. Morawski, Application of carbon-coated TiO_2 for decomposition of methylene blue in a photocatalytic membrane reactor, J. Hazard. Mater. 140 (2007) 369–375.
[11] N. Dubey, S.S. Rayalu, N.K. Labhsetwar, R.R. Naidu, R.V. Chatti, S. Devotta, Photocatalytic properties of zeolite-based materials for the photoreduction of methyl orange, Appl. Catal. A: Gen. 303 (2006) 152–157.
[12] K. Dal, H. Chen, T. Peng, D. Ke, H. Yi, Photocatalytic degradation of methyl orange in aqueous suspension of mesoporous titania nanoparticles, Chemosphere 69 (2007) 1361–1367.
[13] Y. Liu, X. Chen, J. Li, C. Burda, Phtocatalytic degradation of azo dyes by nitrogen-doped TiO_2 nanocatalyst, Chemosphere 61 (2005) 11–18.
[14] V. Druga kumari, M. Subrahmanyam, K.V. Subbax Rao, A. Ratnamala, M. Noorjahan, K. Tanaka, An easy and efficient use of TiO_2 supported HZSM-5 and TiO_2+HZSM-5 zeolite combinate in the photodegradation of aqueous phenol and p-chlorophenol, Appl. Catal. A: Gen. 234 (2002) 155–165.

[15] M.V. Shankar, S. Anandan, N. Venkatachalam, B. Arabindoo, V. Murugesan, Fine route for an efficient removal of 2,4-dichlorophenoxyacetic acid(2,4-D)by zeolite-supported TiO_2, Chemosphere 63 (2006) 1014–1021.
[16] G. Schulz–Ekloff, D. Wohrle, B.V. Duffel, R.A. Schoonheydt, Chromophores in porous silicas and minerals: preparation and optical properties, Microporous Mesoporous Mater. 51 (2002) 91–138.
[17] L.Z. Zhang, P. Cheng, G.-Q. Tang, D.-Z. Liao, Electronic properties of an organic molecule within MCM-41 host: a spectroscopic and theoretical study toward elucidating the variation in band gaps of the guest species, J. Luminescence 104 (2003) 123–129.
[18] A. Corma, Inorganic solid acids and their use in acid-catalyzed hydrocarbon reactions, Chem. Rev. 95 (1995) 559–614.
[19] Q. Cai, Zh-Sh. Luo, W.Q. Pang, Yu-W. Fan, Xi-H. Chen, Fu-Zh. Cui, Dilute solution routes to various controllable morphologies of MCM-41 silica with a basic medium, Chem. Mater. 13 (2001) 258–263.
[20] W. Zeng, Zh. Wang, X.-F. Qian, J. Yin, Z.-K. Zhu, ZnO clusters in situ generated inside mesoporous silica, Mater. Res. Bull. 41 (2006) 1155–1159.
[21] Y. Kayanuma, H. Momiji, Incomplete confinement of electrons and holes in microcrystals, Phys. Rev. B 41 (1990) 10261–10263.
[22] M.A. Zanjanchi, Sh. Asgari, Incorporation of aluminum into the framework of mesoporous MCM-41: the Contribution of diffuse reflectance spectroscopy, Solid State Ionics 171 (2004) 277–282.
[23] A. Corma, H. Garcia, Zeolite-based photocatalysts, Chem. Commun. (2004) 1443–1459.
[24] W.Y. Wang, Y. Ku, Effect of solution pH on the adsorption photocatalyic reaction be haviors of dyes using TiO_2 and Nafion–coated TiO_2, Colloids Surf. A: Physicochem. Eng. Aspects 302 (2007) 261–268.
[25] M.A. Barakat, H. Schaffer, G. Hayes, S. Ismat–Shah, Photocatalytic degradation of 2-chlorophenol by co-doped TiO_2 nanoparticles, Appl. Catal. B: Environ. 7 (2004) 23–30.
[26] C. Wu, X. Liu, D. Wei, J. Fan, J. Wang, Photosonochemical degradation of phenol in water, Water Res. 35 (2001) 3927–3933.
[27] C.C. Wang, C.K. Lee, M.D. Lyu, L.C. Juang, Photocatalytic degradation of C.I. Basic violet 10 using TiO_2 catalysts supported by Y zeolite an investigation of the effects operational parameters, Dyes Pigments 76 (2008) 817–842.
[28] M.V. Phanikrishna Sharma, V. Durgakumari, M. Subrahmanyam, Solar photocatalytic degradation of isoproturon over TiO2/H-MOR composite systems, J. Hazard. Mater 160 (2008) 568–575.